



## OPEN ACCESS

## EDITED BY

Yu Luo,  
Tianjin University, China

## REVIEWED BY

Zhuo-Wei Miao,  
Southeast University, China  
Wei Liu,  
Huawei International Pte Ltd, Singapore

## \*CORRESPONDENCE

Zhenguo Wang,  
✉ coin@ntu.edu.cn  
Weiwei Xu,  
✉ wwwu@nju.edu.cn

RECEIVED 25 May 2023

ACCEPTED 25 August 2023

PUBLISHED 05 September 2023

## CITATION

Yu M, Wang Z, Wang B, Shi J, Liang T-L,  
Jiang R, Zheng K and Xu W (2023), Multi-  
source excited travelling-wave bowtie  
antenna based on a meander series of  
YBCO bicrystal Josephson junctions.  
*Front. Phys.* 11:1228794.  
doi: 10.3389/fphy.2023.1228794

## COPYRIGHT

© 2023 Yu, Wang, Wang, Shi, Liang, Jiang,  
Zheng and Xu. This is an open-access  
article distributed under the terms of the  
[Creative Commons Attribution License  
\(CC BY\)](https://creativecommons.org/licenses/by/4.0/). The use, distribution or  
reproduction in other forums is  
permitted, provided the original author(s)  
and the copyright owner(s) are credited  
and that the original publication in this  
journal is cited, in accordance with  
accepted academic practice. No use,  
distribution or reproduction is permitted  
which does not comply with these terms.

# Multi-source excited travelling-wave bowtie antenna based on a meander series of YBCO bicrystal Josephson junctions

Mei Yu<sup>1,2,3</sup>, Zhenguo Wang<sup>1,2\*</sup>, Bin Wang<sup>4</sup>, Jin Shi<sup>1,2</sup>,  
Tu-Lu Liang<sup>1,2</sup>, Ruirui Jiang<sup>1,2</sup>, Kai Zheng<sup>3,5</sup> and Weiwei Xu<sup>3\*</sup>

<sup>1</sup>School of Information Science and Technology, Nantong University, Nantong, China, <sup>2</sup>Research Center for Intelligent Information Technology, Nantong Key Laboratory of Advanced Microwave Technology, Nantong University, Nantong, China, <sup>3</sup>Research Institute of Superconductor Electronics (RISE), School of Electronic Science and Engineering, Nanjing University, Nanjing, China, <sup>4</sup>Zhongtian Radio Frequency Cable Co, Ltd., Nantong, China, <sup>5</sup>School of Physics and Electronic Electrical Engineering, Huaiyin Normal University, Huaian, China

Series superconducting Josephson junctions (JJs), as terahertz (THz) mixers, have attracted increasing attentions due to their advantages in solving the saturation problem of superconducting mixers, achieving higher mixing harmonics and higher sensitivity in THz band. However, the normal-state resistances of the series JJs are so low that there exists an impedance mismatch between the coupled antenna and the JJs. In this paper, a meander embedding travelling-wave bowtie antenna is proposed for a series of bicrystal JJs. With this antenna, not only the problem of impedance mismatch can be solved, but also more series JJs can be inserted into the antenna. Five and even seven series JJs in the meander match the proposed antenna well. Furthermore, combined current distribution, far-field radiation patterns and parameter study are investigated in the numerical simulation to analyze this antenna.

## KEYWORDS

multi-source excitation, travelling-wave antenna, bowtie antenna, terahertz antenna, series Josephson junctions

## 1 Introduction

Terahertz (THz) communication has its advantages of the high transmission rate, large capacity, strong directivity, high security and good penetration because of its considerable absolute bandwidth. More and more related THz devices [1–4] have been extensively studied. Due to the severe atmospheric attenuation in THz band [5], high requirements are put forward for the effective detection of ultrasensitive THz receivers. In addition, due to the low power consumption and high cost of THz source [6, 7], high-order harmonic mixers become more remarkable for THz receivers to reduce the local oscillator (LO) cost. The larger the number of harmonics, the lower the LO frequency and the cost. High-temperature superconducting (HTS) Josephson junction (JJ) mixers have become good candidates with the advantages of lower cryogenic cost, wide bandwidth, excellent sensitivity, low LO power requirement, large harmonic number and large superconducting energy gap to make them possible to work at higher THz frequencies. Chen *et al.* has accomplished the 490th

harmonic mixing using high- $T_c$  grain boundary (GB) JJ to get THz signal up to 1.6266 THz [8]. This type of JJ was formed by an  $\text{YBa}_2\text{Cu}_3\text{O}_{7-\delta}$  (YBCO) microbridge deposited across a magnesium oxide (MgO) bicrystal boundary.

Typical values of normal-state resistances for YBCO JJs are about 1–40  $\Omega$ . Considering the impedance matching, many works have reported different types of antennas with low impedances for JJ mixers. Du and Gao *et al* integrated and studied the slot antenna for YBCO step-edge JJ mixers [9–13]. Experiments show that the largest harmonic number for YBCO step-edge JJ mixers up to now is 31 at 600 GHz detection. As to YBCO bicrystal JJ mixers, Yu *et al* achieved 46th harmonics with a log-periodic antenna [14], 88th harmonics with a bowtie antenna [15], and 146th harmonics with a novel antenna named bowtie loaded meander antenna [14, 16] at 210 GHz atmospheric window. The increase in the largest harmonic number is caused by the decrease in antenna impedance, thereby improving the coupling efficiency between the JJ and the antenna. Later, Yu *et al* proposed a three-series-bicrystal-JJ mixer and realized 154th harmonics, resulting from the synchronous operation of these three series JJs [17]. However, the impedance mismatch between the antenna and every series JJ still exists and has not been fully solved yet. The harmonic number of series JJ mixer could be further improved if the impedance matching could be ameliorated. The reported antennas applied to the JJs are resonant antennas, which have strict requirements for the positions and the number of the JJs in series, which can be proven in literature [17]. As the meander length increases, only two JJs work synchronously although three JJs are connected in series. Even worse, as more JJs were inserted into the antenna, the characteristic of the antenna would be changed, resulting in the asynchronous operation of the JJs. Compared to resonant antennas, travelling-wave antennas are more suitable for superconducting mixer with more series junctions.

On the other hand, although there are so many attractive characteristics of HTS JJ mixer, it is difficult to manufacture reliable and repeatable JJs with appropriate parameters required for high-performance mixers. Thus, the research progress of HTS THz mixers is lagging behind. When YBCO is immersed in water, the preparation process of multiple photolithography [18, 19] will degrade the sample, resulting in low productivity of the high-performance YBCO JJ mixers. In order to reduce the process steps and improve the sample yield, a simple structure of THz antenna is preferred in the on-chip design, so that the antenna and bicrystal JJs could be integrally formed through only one process in photolithography. In this event, the antenna fabricated with YBCO layer shall not overlap with the GB of the bicrystal boundary to prevent disrupting the formation of JJ.

In short, a suitable antenna should be designed to match the impedances of more series YBCO bicrystal JJs and avoid overlapping with GB in structure. In this paper, we propose a multi-source excited travelling-wave meander embedding bowtie antenna for series JJs. As a result, up to seven JJs have been inserted into the antenna successfully. Numerical simulation shows that five and even seven series JJs in the meander match the antenna well at THz bands. The combined key parameters of the antenna, such as active reflection coefficients, surface current distribution, and far-field radiation patterns, are investigated to further study. In addition, the influence of antenna structure parameters on impedance matching is also discussed.

## 2 Antenna configuration

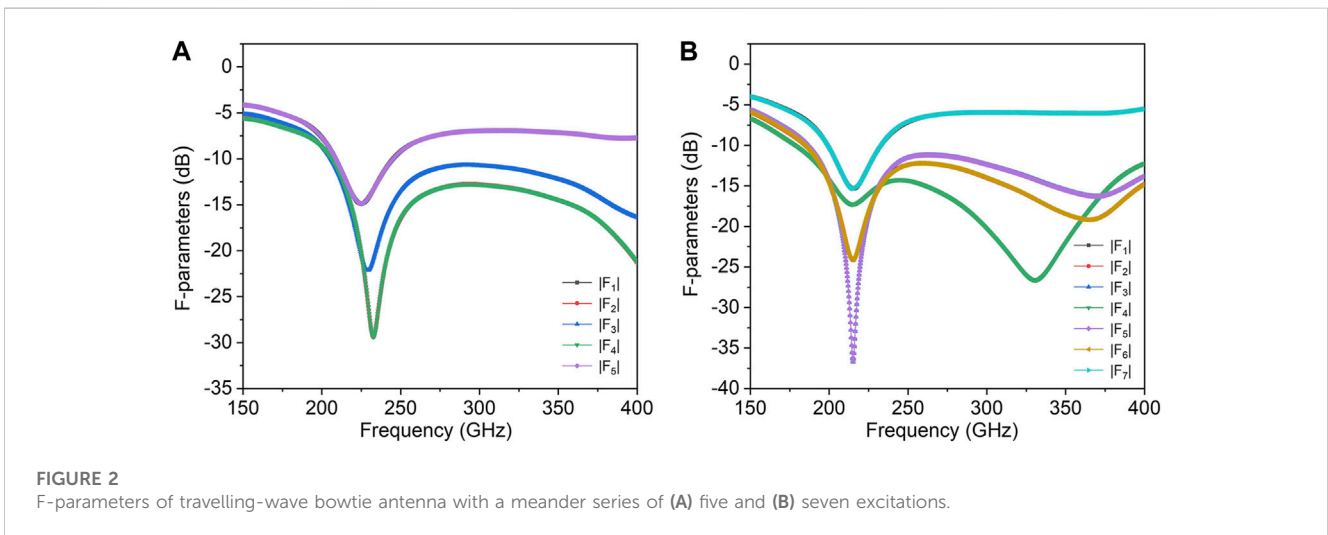
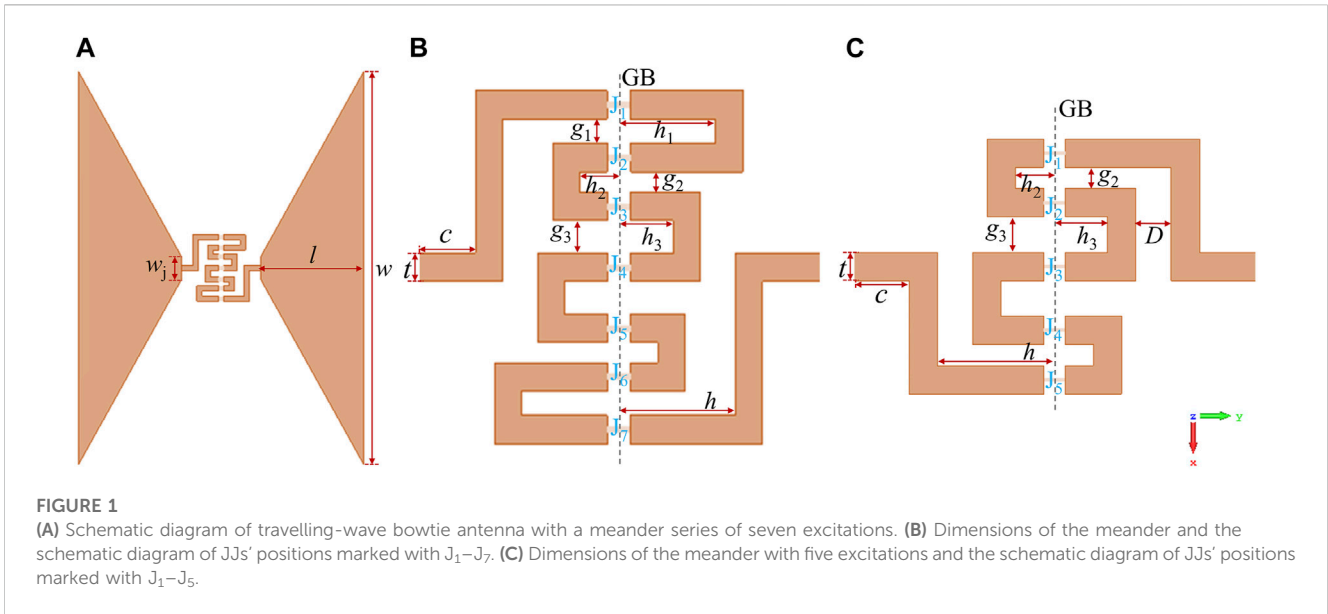
Figure 1A shows the geometry of the travelling-wave bowtie antenna with a meander series of seven excitations. Figure 1B demonstrates an enlarged schematic diagram of the meander in which seven JJs are embedded. Figure 1C shows an enlarged schematic diagram of the meander with five embedded JJs to simultaneously excite the travelling-wave bowtie antenna. The difference between Figures 1B,C is whether there exists a portion related to parameters  $g_1$  and  $h_1$  on both sides of the meander. To ensure the accuracy of the numerical simulation, we selected a commercial software Computer Simulation Technology (CST) Microwave Studio (MWS) to verify the effectiveness of the antenna. In this simulated model, the proposed antenna was placed on a 500- $\mu\text{m}$ -thick MgO substrate with a relative dielectric constant  $\epsilon_r$  of 9.6. Discrete ports with the impedance of 15  $\Omega$  in the meander were used as series elements simulating the JJs.

To form a travelling-wave antenna, the sum of the meander length and the length of the bowtie should be around a guided wavelength  $\lambda_g$ .  $\lambda_g$  equals to  $\lambda_0/\sqrt{(1+\epsilon_r)/2}$ , and  $\lambda_0$  is the wavelength in free space. The JJs are inserted into the center of the meander, which causes the length and spacing of the meander being related to the impedance matching of the travelling-wave bowtie antenna. In this paper, we show one of the dimensions with the parameters of  $l = 135 \mu\text{m}$ ,  $w = 515 \mu\text{m}$ ,  $w_j = 30 \mu\text{m}$ ,  $c = 10 \mu\text{m}$ ,  $t = 4 \mu\text{m}$ ,  $g_1 = g_2 = g_3 = 4 \mu\text{m}$ ,  $h_1 = h_2 = h_3 = 10 \mu\text{m}$  and  $h = 17 \mu\text{m}$  respectively, to study this multi-source excited travelling-wave bowtie antenna at 0.22 THz window [5].

## 3 Antenna characteristics

In the case of simultaneous excitation of several ports, F-parameters, instead of S-parameters, are given in the post-processing results of CST MWS. Figure 2 shows the F-parameters of the travelling-wave bowtie antenna with a meander series of five and seven excitations respectively. Simultaneously excited by five ports with the impedance of 15  $\Omega$ , the antenna matches five series JJs in the meander well with a center frequency of 226 GHz. The 10-dB return loss bandwidth is 16% covering the 0.22 THz window. When the number of the excited ports increases to seven, the center frequency moves down to 216 GHz but the relative bandwidth remains 16%. Thus, it can be seen that as the number of series JJs increases, the length of the meander increases. It results in a downward shift in the center frequency, but the impedance matching keeps a good stability without changing the size of the bowtie and the interval of the meander. In a word, compared to the resonant antenna in the literature [17], the length of the meander in this travelling-wave bowtie antenna can be increased according to the number of JJs in series, and the dimensions of the bowtie on both sides do not need to be readjusted.

Figure 3 shows the instantaneous surface current distribution on the proposed antenna simultaneously fed by five ports at 226 GHz and seven ports at 216 GHz with the phase of  $0^\circ$ ,  $90^\circ$ ,  $180^\circ$ , and  $270^\circ$  respectively. Different from resonant antennas, the



maximum and minimum currents on a travelling-wave antenna move over time. According to [Figure 3A](#), when the antenna is simultaneously excited by five ports with the impedance of  $15 \Omega$  in a meander series, the maximum and minimum surface currents, shown with red and blue arrows on the bowtie respectively, move at different times. In the case of simultaneous excitation of seven ports, [Figure 3B](#) illustrates that, the amplitude of the surface current increases, but the surface current distribution on the bowtie presents the same situation. Therefore, when the bowtie antenna works in a travelling wave, the impedance matching will not be affected at the 0.22 THz window although the number of JJs in the meander series increases.

[Figure 4](#) shows the radiation patterns of the travelling-wave bowtie antenna with a meander series of five and seven excitations at their center frequencies. The patterns are roughly the same, resulting from the uniform surface current distribution. The directivities with five excitations and seven excitations are 7.6 dBi at 226 GHz and 7.4 dBi at 216 GHz respectively.

### 4 Parameter study

To explore the influence of impedance matching between the meander embedding travelling-wave bowtie antenna and a series of JJs, we investigated the parameters of  $t$ ,  $c$ ,  $g_2$ ,  $g_3$ ,  $h_2$ ,  $h_3$ ,  $h$  and  $w$  for simultaneous excitation of five ports. Benefiting from the central symmetric structure of the antenna, the active reflection coefficient at position  $J_1$  equals that at position  $J_5$  ( $|F_1| = |F_5|$ ), which is also applicable at position  $J_2$  and position  $J_4$  ( $|F_2| = |F_4|$ ). Thus, the effects of these parameters on  $|F_1|$ ,  $|F_2|$  and  $|F_3|$  were observed. The increase in active reflection coefficient means that the impedance matching between the antenna and the JJ deteriorates.

[Figure 5](#) shows the simulated  $|F_1|$ ,  $|F_2|$  and  $|F_3|$  of a meander embedding travelling-wave bowtie antenna with variational parameters. And this antenna was excited simultaneously with  $15 \Omega$  at positions  $J_1$ – $J_5$ . Parameter  $t$  is the width of the meander connecting the JJs in series. The  $|F_1|$  decreases when  $t$  increases, and the center frequency remains. Simultaneously, the  $|F_2|$  decreases and

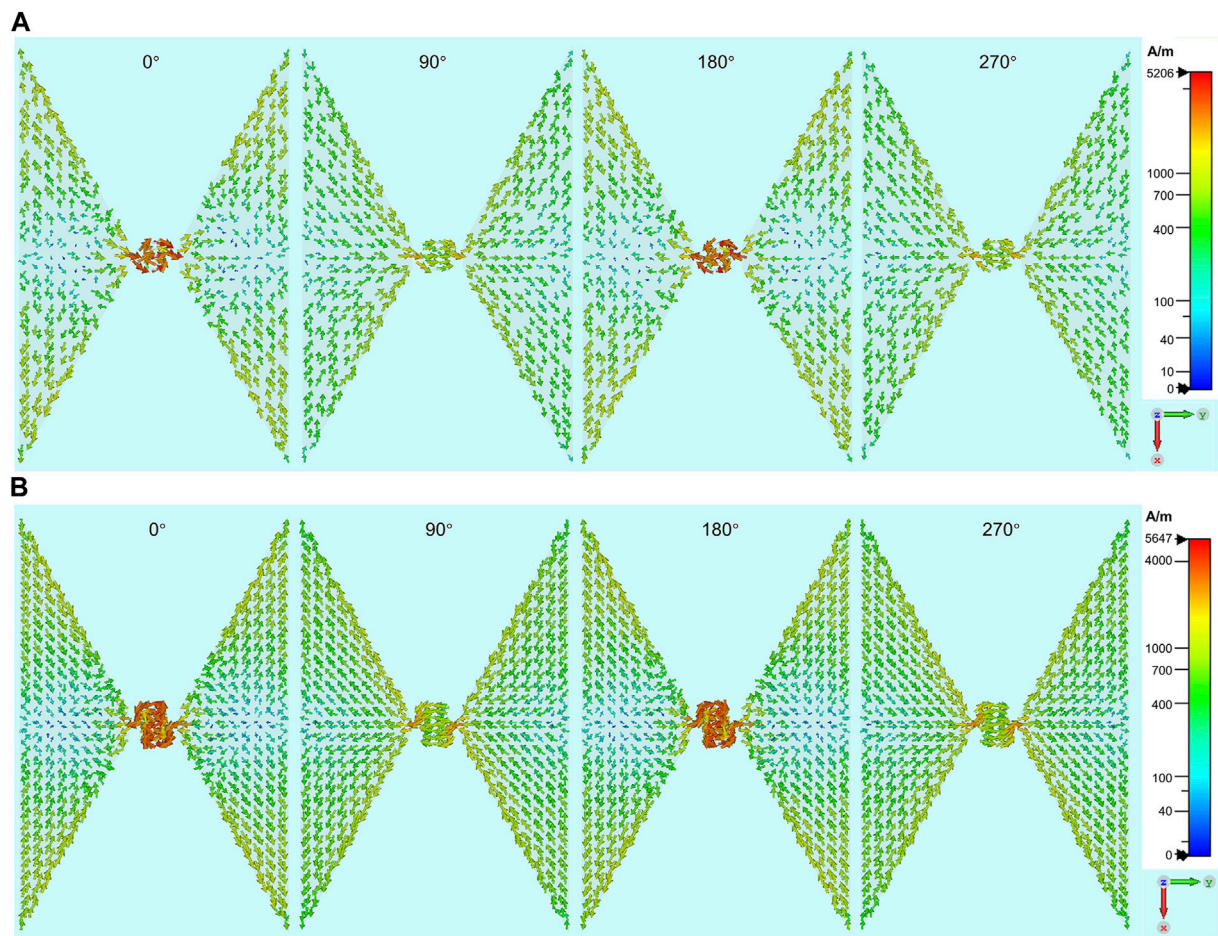


**FIGURE 3** Instantaneous surface current distribution on the proposed antenna simultaneously fed by (A) five ports at 226 GHz and (B) seven ports at 216 GHz with the phase of 0°, 90°, 180°, and 270° respectively.

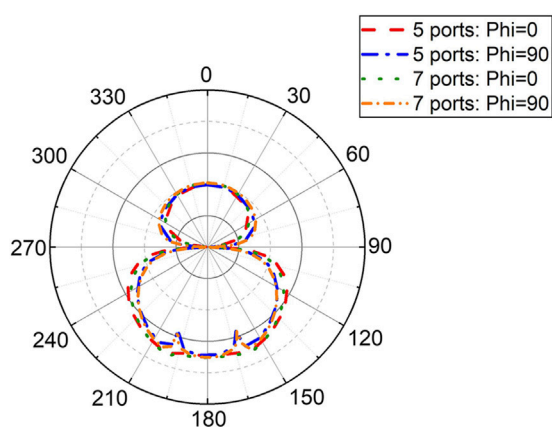
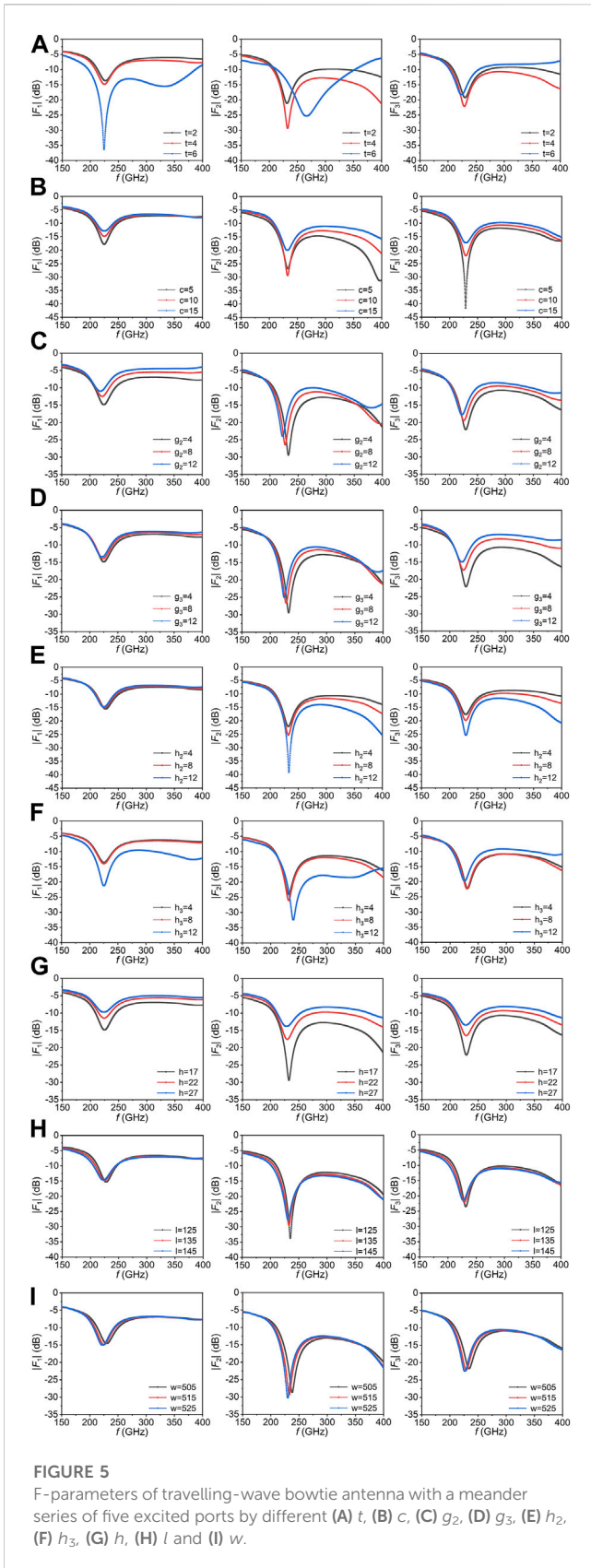


**FIGURE 4** Radiation patterns of travelling-wave bowtie antenna with a meander series of five excited ports at 226 GHz and seven excited ports at 216 GHz.

then increases with an increase of the center frequency, while the  $|F_3|$  decreases and then increases with a decrease of the center frequency. Parameters  $t$  has a significant impact on the impedance matching at every port. This phenomenon may be caused by the coupling between the section bent connecting the bowtie and the section bent connecting the JJs in the meander. This can be seen in Figure 1C, as  $t$  increases, the parameter  $D$  decreases, resulting in a strong coupling. Thus, an optimum value of  $t$  existed to balance the values of  $|F_1|$ ,  $|F_2|$  and  $|F_3|$ .

Parameter  $c$  is the length of a section of meander to connect the bowtie. With the increase of  $c$ , the  $|F_1|$  and the  $|F_2|$  increase while the  $|F_3|$  fluctuates. Thus, the parameter  $c$  should have an optimum value as well. All the center frequencies in  $|F_1|$ ,  $|F_2|$  and  $|F_3|$  are not affected by the change of  $c$ .

Parameters  $g_2$  and  $g_3$  are intervals of the meander. When  $g_2$  and  $g_3$  increase, all the  $|F_1|$ ,  $|F_2|$  and  $|F_3|$  increase. However, the center frequencies of them all decrease. Parameters  $h_2$  and  $h_3$  are lengths in the meander centered around GB. As  $h_2$  increases, the  $|F_1|$  increases with a decrease of the center frequency while the  $|F_2|$



and the  $|F_3|$  decrease with the maintenance of the center frequency. As  $h_3$  increases, the  $|F_1|$  keeps stable firstly and then decreases with a maintenance of the center frequency

while the  $|F_3|$  keeps stable firstly and then increases with a maintenance and subsequent decrease of the center frequency. As for the  $|F_2|$ , it firstly decreases with a maintenance and subsequent increase of the center frequency. Parameter  $h$  is the distance from GB to the section of the meander which is connected to the bowtie. With the increase of  $h$ , the impedance matching between the antenna and the JJs is deteriorating, but their center frequencies maintain. The parameters  $g_2$ ,  $g_3$ ,  $h_2$ ,  $h_3$  and  $h$  are related to the coupling in the meander, thus these five parameters should be well adjusted to achieve good impedance matching.

Parameters  $l$  and  $w$  are the arm length and width of the bowtie respectively. With the increase of  $l$ , the center frequency moves down and the impedance matching deteriorates because all the  $|F_1|$ ,  $|F_2|$  and  $|F_3|$  increase. As  $w$  increases, leading to an increase of the bowtie angle, the center frequency moves down, but the impedance matching shows an improvement trend. However, compared other parameters, parameters  $l$  and  $w$  have little impact on impedance matching.

### 5 Conclusion

A meander embedding travelling-wave bowtie antenna has been presented for series superconducting Josephson junctions (JJs). A suitable model with multi-source excitations in the antenna has been established in the numerical simulation. Combined surface current distribution has been analyzed to survey the operating principle. The F-parameter results indicate that five and even seven series JJs in the meander match the antenna well at THz bands. The experiment has shown that when the bowtie antenna works in a travelling wave mode, the impedance matching will not be affected although more series JJs are inserted into the antenna. The structure parameters related to the meander, which should be carefully designed, are crucial for the impedance matching due to the presence of multi-excitations. Compared to resonant antennas, travelling-wave antennas are more suitable for superconducting mixer with series junctions, because they have a higher tolerance for the number of junctions. This work provides better design solutions and theoretical guidance for the superconducting series-bicrystal-JJ mixer. With this kind of antenna, reported up to 154 harmonics until now in superconducting series-bicrystal-JJ mixer could be further enhanced.

### Data availability statement

The original contributions presented in the study are included in the article/Supplementary Material, further inquiries can be directed to the corresponding authors.

### Author contributions

Conceptualization, MY, BW, and WX; formal analysis, MY, ZW, and T-LL; investigation, BW, T-LL, RJ, and KZ; methodology, MY, JS, and RJ; project administration, MY, KZ, and WX;

writing—original draft, MY, ZW, and KZ; writing—review and editing, MY, ZW, and WX. All authors contributed to the article and approved the submitted version.

## Funding

This work was supported by the National Natural Science Foundation of China under the grant numbers of 62104117 and 62201223, the Innovation Program for Quantum Science and Technology under the grant number of 2021ZD0301701, the Natural Science Foundation of the Jiangsu Higher Education Institutions of China under the grant number of 21KJB510047, and the Nantong Science and Technology Plan Project under the grant number of JB2021006.

## References

- Sun H, Wieland R, Xu Z, Qi Z, Lv Y, Huang Y, et al. Compact high- $T_c$  superconducting terahertz emitter operating up to 86 K. *Phys Rev Appl* (2018) 10:024041. doi:10.1103/physrevapplied.10.024041
- Su RF, Zhang YD, Tu X, Jia X, Kang L, Jin BB, et al. Terahertz direct detectors based on superconducting hot electron bolometers with different biasing methods. *IEEE Trans Appl Supercond* (2019) 29(5):1–4. doi:10.1109/tasc.2019.2906785
- Li C, Li W, Duan S, Wu J, Chen B, Yang S, et al. Electrically tunable electromagnetically induced transparency in superconducting terahertz metamaterials. *Appl Phys Lett* (2021) 119:052602. doi:10.1063/5.0056489
- Li C, Jiang L, Ma Q, Teng Y, Bian B, Yu M, et al. Electrically tunable terahertz switch based on superconducting subwavelength hole arrays. *Appl Opt* (2021) 60(25):7530–5. doi:10.1364/ao.435569
- Yang Y, Shutler A, Grischkowsky D. Measurement of the transmission of the atmosphere from 0.2 to 2 THz. *Opt Express* (2011) 19(9):8830–8. doi:10.1364/oe.19.008830
- An DY, Yuan J, Kinev N, Li MY, Huang Y, Ji M, et al. Terahertz emission and detection both based on high- $T_c$  superconductors: towards an integrated receiver. *Appl Phys Lett* (2013) 102:092601. doi:10.1063/1.4794072
- Krasnov MM, Novikova ND, Cattaneo R, Kalenyuk AA, Krasnov VM. Design aspects of  $\text{Bi}_2\text{Sr}_2\text{CaCu}_2\text{O}_{8+\delta}$  THz sources: optimization of thermal and radiative properties. *Beilstein J Nanotechnol* (2021) 12:1392–403. doi:10.3762/bjnano.12.103
- Chen J, Myoren H, Nakajima K, Yamashita T. THz mixing properties of  $\text{YBa}_2\text{Cu}_3\text{O}_{7-\delta}$  grain boundary Josephson junctions on bicrystal substrates. *Phys C* (1997) 293:288–91. doi:10.1016/s0921-4534(97)01559-1
- Du J, Weily AR, Gao X, Zhang T, Foley CP, Guo YJ. HTS step-edge Josephson junction terahertz harmonic mixer. *Supercond Sci Technol* (2017) 30(2):024002. doi:10.1088/0953-2048/30/2/024002
- Du J, Pegrum CM, Gao X, Weily AR, Zhang T, Guo YJ, et al. Harmonic mixing using a HTS step-edge Josephson junction at 0.6 THz frequency. *IEEE Trans Appl Supercond* (2017) 27(4):1–5. doi:10.1109/tasc.2016.2636081
- Gao X, Zhang T, Du J, Weily AR, Guo YJ, Foley CP. A wideband terahertz high- $T_c$  superconducting Josephson-junction mixer: electromagnetic design, analysis and characterization. *Supercond Sci Technol* (2017) 30(9):095011. doi:10.1088/1361-6668/aa7ccl
- Gao X, Du J, Zhang T, Guo YJ, Foley CP. Experimental investigation of a broadband high-temperature superconducting terahertz mixer operating at temperatures between 40 and 77 K. *J Infrared Milli Thz Waves* (2017) 38:1357–67. doi:10.1007/s10762-017-0422-x
- Gao X, Zhang T, Du J, Guo YJ. Design, modelling and simulation of a monolithic high- $T_c$  superconducting terahertz mixer. *Supercond Sci Technol* (2018) 31(11):115010. doi:10.1088/1361-6668/aade5b
- Yu M, Geng H, Gao X, Hua T, Chen W, Shi J, et al. Grain boundary Josephson junction harmonic mixer coupled with a bowtie loaded meander antenna with zero-bias operation. *IEEE Trans Appl Supercond* (2019) 29(8):1–4. doi:10.1109/tasc.2019.2951120
- Yu M, Li C, Gao X, Wang Z, Liang T-L, Shi J, et al. High- $T_c$  superconducting Josephson junction harmonic mixers with stub tuners on integrated bowtie antennas. *Appl Sci* (2022) 12(24):12813. doi:10.3390/app122412813
- Yu M, Geng H, Jiang S, Hua T, An D, Xu W, et al. Bowtie loaded meander antenna for a high-temperature superconducting terahertz detector and its characterization by the Josephson effect. *Opt Express* (2020) 28(10):14271–9. doi:10.1364/oe.390997
- Yu M, Geng HF, Hua T, An DY, Xu WW, Chen ZN, et al. Series YBCO grain boundary Josephson junctions as a terahertz harmonic mixer. *Supercond Sci Technol* (2020) 30(2):025001. doi:10.1088/1361-6668/ab5e13
- Du J, Hellicar AD, Leslie KE, Nikolic N, Hanham SM, Macfarlane JC, et al. Towards large scale HTS Josephson detector arrays for THz imaging. *Supercond Sci Technol* (2013) 26(11):115012. doi:10.1088/0953-2048/26/11/115012
- Malnou M, Feuillet-Palma C, Ulysse C, Faini G, Febvre P, Sirena M, et al. High- $T_c$  superconducting Josephson mixers for terahertz heterodyne detection. *J Appl Phys* (2014) 116(7):074505. doi:10.1063/1.4892940

## Conflict of interest

BW was employed by Zhongtian Radio Frequency Cable Co, Ltd. The remaining authors declare that the research was conducted in the absence of any commercial or financial relationships that could be construed as a potential conflict of interest.

## Publisher's note

All claims expressed in this article are solely those of the authors and do not necessarily represent those of their affiliated organizations, or those of the publisher, the editors and the reviewers. Any product that may be evaluated in this article, or claim that may be made by its manufacturer, is not guaranteed or endorsed by the publisher.